PROCEEDINGS OF SCIENCE

Investigating the nature of TeV gamma-ray variability in blazars

Vardan Baghmanyan,[a,*] **Lenz Oswald,**[a] **Leonard Pfeiffer,**[a] **Alessandra Azzollini,**[a] **Eleonora Barbano,**[a] **Gaëtan Fichet de Clairfontaine**[a] **and Sara Buson**[a]

[a] *Julius-Maximilians-Universität Würzburg, Fakultät für Physik und Astronomie, Emil-Fischer-Str. 31, D-97074 Würzburg, Germany*

E-mail: vardan.baghmanyan@uni-wuerzburg.de

One of the most remarkable characteristics of blazars is their highly variable and luminous emission across the entire electromagnetic spectrum, including very high energy (VHE) gamma rays. Specifically, the TeV gamma-ray variability is a powerful probe of the physical processes in the innermost regions of the jet that constrains the models of particle acceleration and radiation in these extreme environments. Despite the discovery of dozens of blazars with ground-based TeV gamma-ray telescopes in recent decades, the origin of VHE gamma-ray emissions remains unclear.

In this work, we investigate the TeV variability properties of three BL Lac objects: PKS 2155-304, Mrk 421, and Mrk 501, by analyzing the data collected by the MAGIC, H.E.S.S., and VERITAS telescopes over the last two decades. In contrast to previous studies, we employ the same methodology using the Bayesian blocks and the Eisenstein-Hut HOP algorithm to investigate the TeV variability of these BL Lac objects. This consistent framework is intended to enable a comprehensive analysis of the temporal properties and yield deeper insights into the physical mechanisms that may underlie the observed flux variability.

38th International Cosmic Ray Conference (ICRC2023)
26 July - 3 August, 2023
Nagoya, Japan

*Speaker

PoS(ICRC2023)921

1. Introduction

Blazars are a unique class of active galactic nuclei (AGNs) characterized by the presence of relativistic jets pointing directly toward the observer. The broadband spectral energy distribution (SED) of blazars exhibits distinct features, typically displaying a characteristic double-bump structure from radio up to very high energy (VHE) γ-rays. It is generally accepted that the low-energy bump originates from the synchrotron radiation of primary relativistic electrons in the jet, while the high-energy bump is thought to arise by Inverse Compton (IC) scattering from the self-produced synchrotron photons (SSC) or external thermal photons (SEC). The simplest, one-zone, version of this model assumes that both bumps originate from a single site in the jet, and while explaining the blazar multiwavelength SEDs in most cases, there are some challenges. In particular, the leptonic one-zone model faces difficulties in explaining the large separation between synchrotron and γ-ray peaks, HE γ-ray emission, rapid variability, and multiwavelength correlations observed in blazars [1–4]. Moreover, in some cases, both leptonic and hadronic frameworks describe the same SED reasonably, which favors the possibility of hadronic models [5].

The emission variability of blazars is one of the most powerful tools for constraining physical models. Namely, the variability timescales provide valuable insights into the size and location of the emitting region, while the flux measurement helps determine the energy content at the emission site. In this context, the TeV gamma-ray variability of blazars is of particular interest as it allows for the study of the most energetic particles and provides more precise constraints on the physical parameters involved. Furthermore, for BL Lac objects, the VHE spectrum is of crucial importance since they emit a significant portion of their overall radiation in the TeV energy range.

2. Source and Data Selection

In this study, our focus was on investigating the blazars PKS 2155-304, Mrk 501, and Mrk 421. These particular BL Lac objects have been extensively studied by the imaging atmospheric Cherenkov telescopes (IACTs) due to their notable variability and exceptionally high flux during intense flaring events. We used observational data from the most prominent IACT observatories, namely HESS, MAGIC, and VERITAS, which have been observing these blazars for the past two decades, covering both weekly-monthly and intra-day observations.

We have collected data from the papers published by the respective collaborations. However, in this paper, we focus specifically on presenting the data that show significant variability based on the methodology outlined in the next section. Specifically, the references for the data used in this work are as follows: [7, 13–18, 20–22].

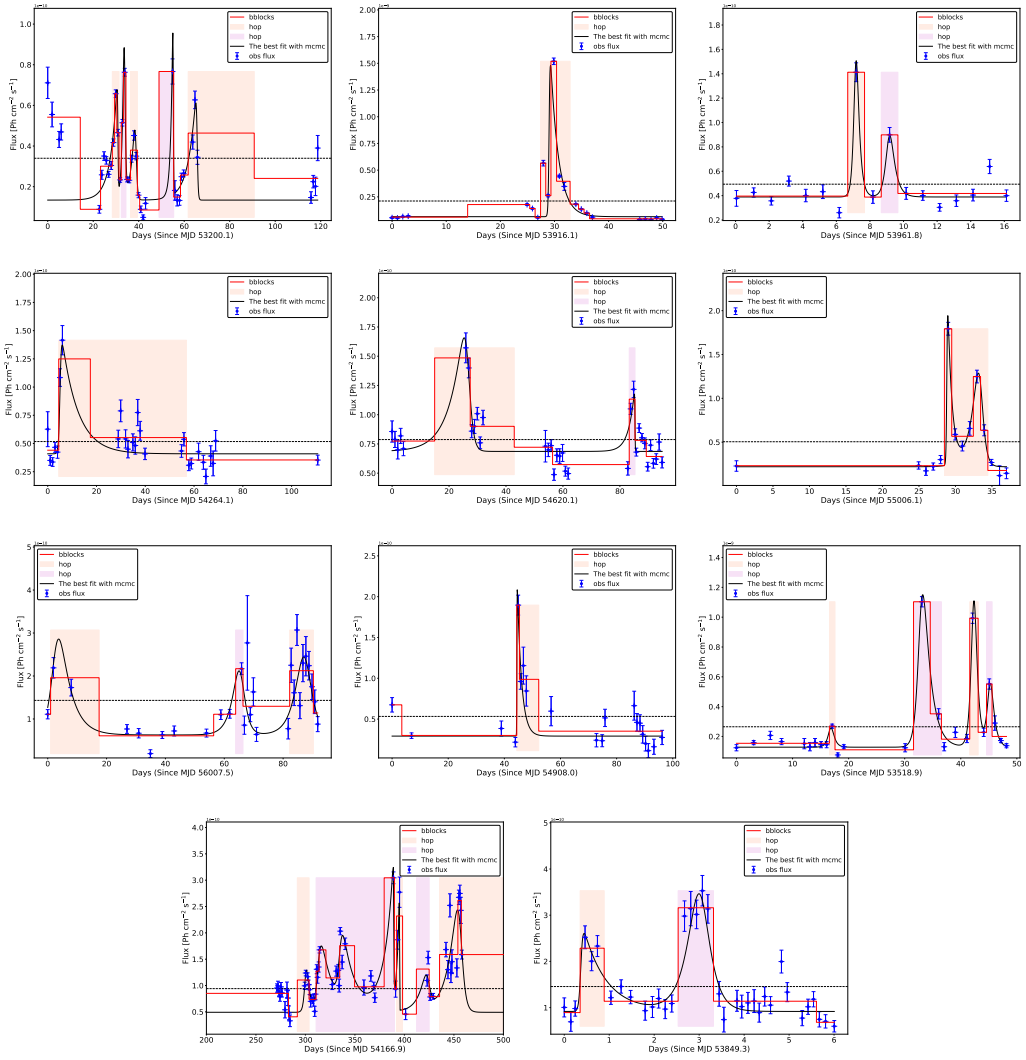

Figure 1: The weekly-monthly TeV light curves of PKS 2155-304 (two upper panels [13]), Mrk 501 (third panel [16–18]), and Mrk 421 (fourth panel [7, 22]) are shown with the Bayesian block representation depicted in red. The shaded regions highlight the identified HOP groups, indicating distinct periods of heightened activity. The dashed black line represents the average flux level across the observation period. Exponential flare profiles, represented by solid black lines, show the fit to the HOP groups.

3. Methodology

For the purpose of this work, first, we generate a block-wise constant representation of sequential light curves by identifying statistically significant variations using the Bayesian Block (BB) algorithm [6], which works by maximizing the signal-to-noise ratio. One of the advantages of this method is that it also works on unevenly sampled data with gaps which is very common for the TeV light curves of blazars. Also, it is a non-parametric

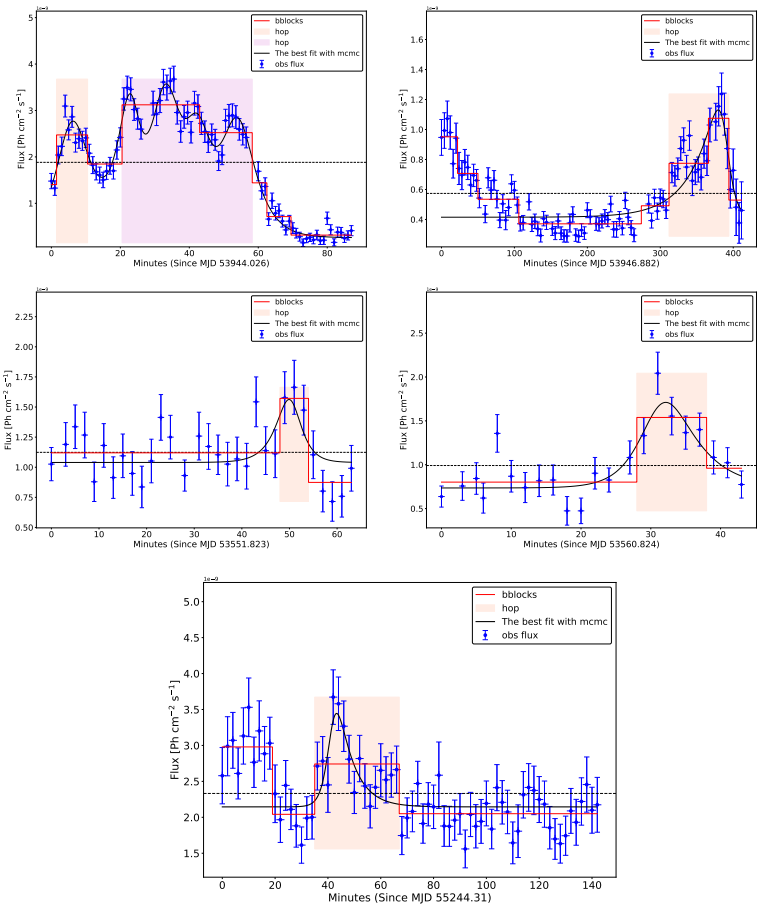

Figure 2: The intra-day TeV light curves of PKS 2155-304 (upper panel [14, 15]), Mrk 501 (middle panel [20]), and Mrk 421 (lower panel [21]) with an identical representation as in Figure 1.

technique, meaning that it does not make any assumptions about the underlying distribution of the data. The segmentation of the light curve can be controlled by the false-positive rate probability, which quantifies the probability of false detection of a flare in the observed data. In this study, we used a 3σ threshold to identify flares in the TeV light curves. This method has been already used in the TeV band to identify flares or different levels of variability in AGNs [7–9].

To characterize the flares, we applied the HOP algorithm [10] on the block representations of the light curves generated by the BB algorithm. This creates so-called HOP groups of consecutive BBs, which are treated as flare episodes. The determination of the start and end of the HOP groups relies on the flux exceeding or dropping below a predefined flux level. Specifically, we use the average flux for the given period as our reference level. To minimize potential bias caused by substantial changes in the average flux, applying the HOP algorithm for each observation period is crucial, ensuring accurate and unbiased identification of the groups.

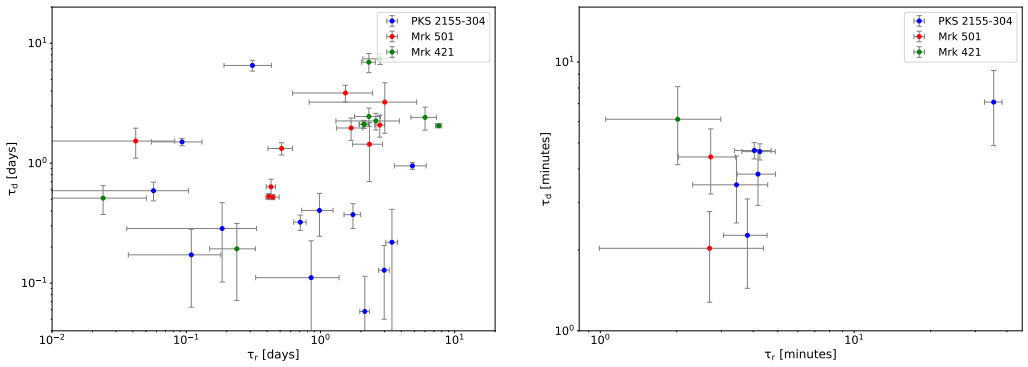

Figure 3: Distribution of rise and decay times for flare profiles fitted to the data, separated into weekly-monthly (left) and intra-day (right) time scales.

As was shown by [11], the combination of BB and the HOP algorithm provides an objective way to split a γ-ray light curve into groups of steady and flaring episodes. The implemented of these algorithms for this procedure is available on GitHub. Finally, we fitted each HOP group i with a sum of exponential profiles following the procedure described in [11]. Specifically, the function is defined as

$$F_{\rm flare,i}(t) = F_{\rm base} + \sum_{i=1}^{N_{\rm HOP}} F_{0,ij} \times \left[\exp\left(\frac{t - t_{0,ij}}{\tau_{\rm rise,ij}}\right) + \exp\left(\frac{t_{0,ij} - t}{\tau_{\rm decay,ij}}\right) \right]^{-1} \quad (1)$$

where $F_{\rm base}$ represents the baseline level, while $F_{0,ij}/2$ measures the flare amplitude. $t_{0,ij}$ is the approximate peak time, and $\tau_{\rm rise,ij}$ and $\tau_{\rm decay,ij}$ represent the rise and decay timescales of the flares, respectively. To determine the parameters of the flaring profiles and their corresponding uncertainties, we employed the Markov Chain Monte Carlo (MCMC) method using the non-linear optimization LMFIT package and the emcee tool [12]. The number of flare profiles considered in the fitting for each HOP was determined based on the Akaike information criterion (AIC). If the difference between the two AIC values, represented as $\Delta AIC = \Delta AIC_{n=2} - \Delta AIC_{n=1}$, was less than zero ($\Delta AIC < 0$), two flare profiles were selected.

4. Results

In this section, we present the results obtained from the BB and HOP algorithms, along with the fitting of the flaring profiles and estimation of the size and location of the emission region. Specifically, Figures 1 and 2 show the light curves with exponential fits of the identified flare profiles for the weekly-monthly and intra-day time scales, respectively. Overall, the identified flare profiles have successfully described the evolution of the light

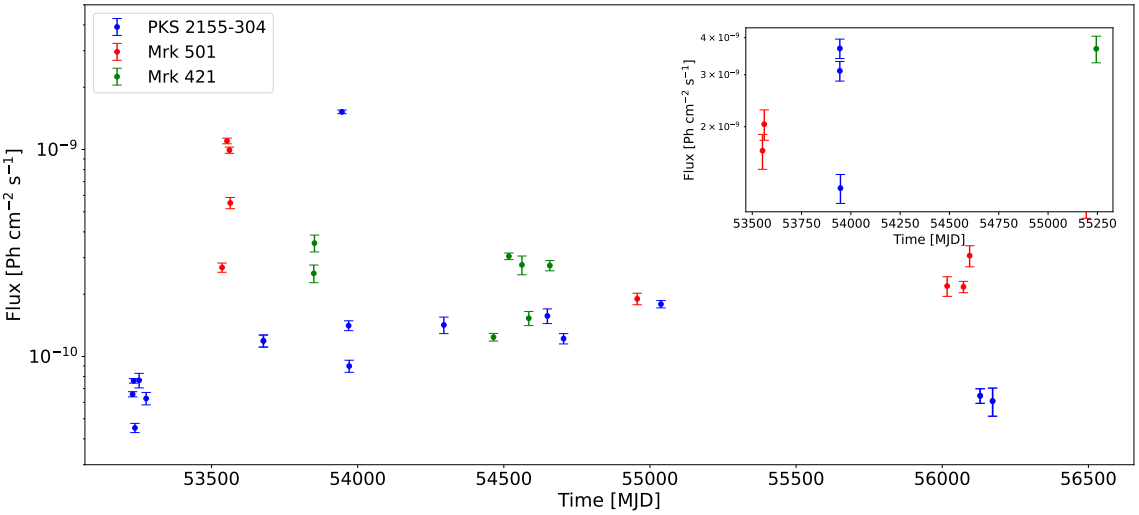

Figure 4: Observed maximum fluxes for the identified HOPs group presented with time represented as the center of each group. The inset displays the fluxes derived from intraday light curves.

curve, enabling an accurate description of the most flare properties. The corresponding rise and decay times, along with their uncertainties, are presented in Figure 3. The flux variability timescales can be used to constrain the size and the location of the emission region. Rapid variability observed in TeV γ-ray indicates the size of the emission region to be of few Schwarzschild radii of the central black hole and hence should be located close to the central engine.

Specifically, the size of the emitting region can be constrained by $R \lesssim \delta c t_{var}^{obs} \simeq 8 \times 10^{-3}\,(\delta/10)\,\left(t_{var}^{obs}/1\,d\right)$ pc, where $t_{var}^{obs} = min(\tau_{rise}, \tau_{decay})$ is the minimum variability time of the flare and δ is the Doppler factor. Assuming $\delta = 30$, we find that the size of the emitting region assuming the variabilities on the daily scales are always below 0.1 pc reaching up to $10^{-5} - 10^{-4}$ parsec scales for the minute times scale variabilities. We note that the derived constraints from the minute time scale variabilities are in the same order as the Schwarzschild radii $9.6 \times 10^{-5} - 1.9 \times 10^{-4}$ pc, $8.6 \times 10^{-5} - 3.3 \times 10^{-4}$ pc and $1.9 \times 10^{-5} - 8.6 \times 10^{-5}$ pc, respectively for PKS 2155-304, Mrk 501 and Mrk 421.

Similarly, the location of the emission site can be constrained by $d \lesssim 2c\Gamma^2 t_{var}^{obs} \simeq 0.04\,(\delta/10)^2\,\left(t_{var}^{obs}/1\,d\right)\ pc\ (\delta \simeq 2\Gamma)$ assuming a conical jet scenario, where the jet inclination angle in respect to the observer is assumed to be 0 ($\delta \simeq 2\Gamma$). For the daily variability time scales, assuming $\delta = 30$, the location of the emission region is estimated to be within 1 pc from the central engine. For the minute time scale variabilities, the constraints go up to $5 \times 10^{-4} - 2 \times 10^{-3}$ pc scales.

The light curves shown in Figure 4 is derived from the maximum flux values of the identified HOP groups for each source, where the time is defined as the center of the group. By excluding the fluxes associated with the exceptional flaring activities detected from PKS 2155-304 and Mrk 501 [14, 15, 20], it becomes evident that the maximum

fluxes for Mrk 421 and Mrk 501, which have similar red shifts, are at the same levels, i.e., 1×10^{-11} cm^{-2} s^{-1} and 2×10^{-11} cm^{-2} s^{-1}, respectively. The maximum fluxes of the identified HOP groups for PKS 2155-304 are in the range of $(4.5 - 18) \times 10^{-11}$ cm^{-2} s^{-1}.

5. Conclusion

Our study presents preliminary findings from the analysis of temporal data for three TeV BL Lac objects: Mrk 421, Mrk 501, and PKS 2155-304. We used advanced algorithms (BB and HOP) to detect significant flaring events and investigate their variability characteristics. Our research is still in progress and will encompass a broader range of blazars in the TeV sky to explore their potential variability. Furthermore, we plan to include X-ray and GeV γ-ray light curves, aiming to enhance our understanding of the origin of emission variability in blazar jets.

6. Acknowledgements

Funded by the Deutsche Forschungsgemeinschaft (DFG, German Research Foundation) – Project-ID 443220636.

References

[1] Ghisellini, G. & Tavecchio, F. 2009, , 397, 985.

[2] Barkov, M. V., Aharonian, F. A., Bogovalov, S. V., et al. 2012, , 749, 119.

[3] Ghisellini, G., Maraschi, L., & Tavecchio, F. 2009, , 396, L105.

[4] Böttcher, M. 2007, , 309, 95.

[5] Abdo, A. A., Ackermann, M., Ajello, M., et al. 2011, , 736, 131.

[6] Scargle, J. D., Norris, J. P., Jackson, B., et al. 2013, , 764, 167.

[7] Ahnen, M. L., Ansoldi, S., Antonelli, L. A., et al. 2016, , 593, A91.

[8] Feng, Q. & VERITAS Collaboration 2022, 37th International Cosmic Ray Conference, 802.

[9] H. E. S. S. Collaboration, :, Aharonian, F., et al. 2023, arXiv:2305.09607.

[10] Eisenstein, D. J. & Hut, P. 1998, , 498, 137.

[11] Meyer, M., Scargle, J. D., & Blandford, R. D. 2019, , 877, 39.

[12] Foreman-Mackey, D., Hogg, D. W., Lang, D., et al. 2013, , 125, 306.

[13] H. E. S. S. Collaboration, Abdalla, H., Abramowski, A., et al. 2017, , 598, A39.

[14] Aharonian, F., Akhperjanian, A. G., Bazer-Bachi, A. R., et al. 2007, , 664, L71.

[15] H. E. S. S. Collaboration, Abramowski, A., Acero, F., et al. 2010, , 520, A83.

[16] Ahnen, M. L., Ansoldi, S., Antonelli, L. A., et al. 2018, , 620, A181.

[17] Ahnen, M. L., Ansoldi, S., Antonelli, L. A., et al. 2017, , 603, A31.

[18] Albert, J., Aliu, E., Anderhub, H., et al. 2007, , 669, 862.

[19] Furniss, A., Noda, K., Boggs, S., et al. 2015, , 812, 65.

[20] MAGIC Collaboration, Acciari, V. A., Ansoldi, S., et al. 2020, , 637, A86.

[21] Abeysekara, A. U., Benbow, W., Bird, R., et al. 2020, , 890, 97.

[22] Aleksić, J., Anderhub, H., Antonelli, L. A., et al. 2010, , 519, A32.

[23] Barth, A. J., Ho, L. C., & Sargent, W. L. W. 2002, , 566, L13.

[24] Zhang, Z., Gupta, A. C., Gaur, H., et al. 2019, , 884, 125.